Prototyping FOURIER: the first generation near-infrared science beam combiner at the MROI

Mortimer D.[a] and Buscher D.[a]

[a]Cavendish Laboratory, University of Cambridge, 19 J J Thompson Avenue, Cambridge, CB3 0HE, UK

ABSTRACT

The Magdalena Ridge Observatory Interferometer (MROI) is currently under construction in New Mexico at an altitude of 3.2 km. When completed it will consist of ten 1.4 m telescopes and will operate at wavelengths from 0.6 to 2.4 μm. Here we present the preliminary design of the Free-space Optical multi-apertUre combineR for IntERferometry (FOURIER), the first generation near-infrared science beam combiner at the MROI which is currently under development. The combiner will operate in the J, H and K bands and combine three beams from the currently funded subset of three telescopes. The primary aim of the combiner is to achieve high sensitivity leading to its unique design.

Keywords: interferometry, near-infrared, beam combiner, MROI

1. INTRODUCTION

The MROI project is working towards measuring visibilities and closure phases on the funded three telescope configuration. To support this the development of a near-infrared (NIR) science combiner is required.

A NIR combiner is being prioritized as the first instrument to come online for two primary reasons. The first reason is due to atmospheric seeing: deterioration of the incoming wavefronts becomes rapidly harder to compensate for at visible wavelengths meaning tolerances for the observatory during the initial phase need not be as strict. The second reason is that in the J, H and K bands many of the top level science targets are intrinsically bright.

2. SCIENTIFIC MOTIVATION

FOURIER will initially operate on baselines between 8-40m that will first be implemented at the MROI. While the initial baseline length will not push the boundaries beyond what is currently attainable at other interferometers FOURIER will make advances on two different fronts. Firstly in sensitivity, the final goal for the MROI is to reach 14th magnitude in the H band which will open up access to many more targets of a particular class whereas currently only the brightest are observable with other arrays, for example with AGNs. The second front is FOURIER's extensive simultaneous wavelength coverage. With the current design FOURIER will be able to pass the J, H and K bands simultaneously.

2.1 Initial Science Cases

The initial observing campaigns for FOURIER will be limited to more 'classical' interferometric targets such as giant stars and binary systems. One class of giant stars that will be of particular interest are Mira variables. Miras are asymptotic giant branch stars which exhibit periods of order hundreds of days.[1] While models exist to explain the variabilities in the photospheric radius and atmospheric molecular layers[2,3] the environments around Mira stars are not strongly constrained by observations.[4] A couple of particularly pertinent questions are how the molecular layers change during the pulsation period and whether the changes are in phase or out of phase with respect to each other.

(Send correspondence to Mortimer D)
Mortimer D: E-mail: djm244@cam.ac.uk,
Buscher D: E-mail: dfb@mrao.cam.ac.uk

With Fourier's large simultaneous wavelength coverage it will be able to measure high accuracy relative visibilities across the J, H and K bands which will allow for tighter constraints on processes in Mira atmospheres. When the MROI reaches three telescopes studies of the asymmetries around Miras will allow for further constraints to be derived.

2.2 Future Science Cases

Beyond the initial phase of the MROI, when longer baselines and greater UV coverage are available there are many science cases that FOURIER or a future combiner based on FOURIER will explore. Below are two of the high priority areas of research with which the MROI and a FOURIER like combiner will be able to push the boundaries with its high sensitivity and large wavelength coverage.

2.2.1 Active Galactic Nuclei

The driver for the MROIs unprecedented sensitivity aim is the AGN science case. To date few AGN have been accessible to optical interferometers owing to their high magnitudes, resulting in only of order a dozen or so being observed with current optical interferometers. The MROIs final goal of H band sensitivity down to 14th magnitude will allow observations of order 100 AGN.[5]

The goal of the MROI is to probe the unified scheme of AGN[6] at near-infrared wavelengths. Studies in the mid-infrared have already begun to show that the unified scheme may not be able to explain interferometric observations, for example interferometric data suggests that warm dust emission predicted by the classical AGN unified scheme to be housed in the obscuring dust torus may in fact extend in the polar direction.[7] Observations in the near-infrared so far have been even more limited[8] as the difficulty of acquiring fringes due to the typical brightness of AGN is compounded by the faster changing atmospheric conditions at near-infrared wavelengths[9,10] however by studying the morphology of large numbers of AGN through model independent imaging the MROI aims to significantly increase the wealth of observations at near-infrared wavelengths.

2.2.2 Young Stellar Objects

A great deal of work by many prominent people in the field has been done on YSOs, and yet we are stuck. Progress has been hampered due to a few reasons, one being that YSOs are deeply embedded objects resulting in high extinctions. A second reason that affects the study of intermediate and high mass YSOs is that they form in significantly smaller numbers than their lower mass T-Tauri cousins as described by the initial mass function resulting in intermediate and high mass YSOs being found at greater distances. These factors result in the majority of targets being faint, making it difficult to acquire fringes.

An unresolved question in the field of YSOs is the interaction of the star with its circumstellar disk in the intermediate and higher mass range. Optical interferometry is well placed to study these interactions however as the resolution allows the inner few AU to be resolved in many cases[11–13] see Kraus (2015)[14] for a review.

Near-infrared wavelengths are sensitive to warm dust around the inner few AU of YSOs where many complex processes take place, primarily due to interactions of the circumstellar environment with the star itself. Recent spectroscopic surveys such as Fairlamb et al 2017[15] have made significant progress in the field but lack spatial information, relying on modelling of the physical structures to interpret results. Spectroscopic surveys have however demonstrated the power of conducting large statistical surveys of a given class of objects. In this case probing for relations such as accretion rate against fundamental parameters such as stellar temperature. Large scale statistical surveys of YSOs with optical interferometers is now becoming possible[16] thanks to advances in sensitivity allowing access to more targets. The sensitivity attainable by the MROI will allow this kind of statistical work to further continue.

Another way a future FOURIER-like combiner will make progress in this field will be with its simultaneous J, H and K band coverage. Compared to most current beam combiners this is an increase in simultaneous wavelength coverage. Large wavelength coverage allows for the spatial origin of a wider range of black body temperatures to be extracted which will probe (amongst other things) the radial temperature dependence of the circumstellar disk and if this varies as a function of system parameters such as accretion rate. The potential insights these kinds of studies can provide could aid in solving the so called undersized Herbig Be problem.[17] As has been outlined, With the resolution, bandpass and increased number of observable targets a FOURIER-like combiner will be well placed to study the inner regions of YSO circumstellar disks.

3. UNIQUE REQUIREMENTS FOR FOURIER

The top priority for the MROI is to reach unprecedented sensitivity. To achieve its science goals the MROI is required to reach 14th magnitude in the H band.[5] This has led to a design where a high throughput is the top design priority. After consideration of this and other requirements The following specifications were prioritised:

- Strictly optimised for sensitivity
- Simultaneous J, H and K band coverage
- Low resolution spectral dispersion mode

The design presented here is a three-way image plane free space combiner. Wherever possible reflective components have been utilised rather than transmissive ones, primarily as reflective components allows for a more achromatic solution to be found which is of high importance to be able to pass the J, H and K bands simultaneously.

Because interactions with every optic in the system have associated reflection, transmission and scattering losses, the number of components was minimized, resulting in the design presented here where the incoming beams undergo two reflections and three transmissions from arriving at the beam combiner to reaching the CCD. This is a significant reduction in complexity over typical current generation beam combiners. However this comes at a cost of reducing the combiner to relatively basic functionality.

For example spatial filtering in FOURIER will be carried out in the spectral dispersion direction by a slit at the focus of the initial parabolic mirror (M1). Spatial filtering in the fringe direction will be applied via software. A slit was opted for rather than single mode fibers primarily to increase throughput of the combiner as there is no coupling loss or loss of light that does not match the fundamental mode of the fiber. A secondary advantage to using a slit (resulting in a free space design) is that FOURIER is not limited to passing only the wavelengths that available fibers can transmit. Hence it is possible to pass the J, H and K bands simultaneously.

In the past decade spectro-interferometry has revolutionised the capabilities of optical interferometers. Allowing advances on the instrumentation side by reducing bandwidth smearing, increasing the coherence length, and on the science side by opening up a range of new possibilities such as such as characterising the spectral index of a target, allowing black body temperatures to be derived,[16] or in the case of high spectral dispersion ($R > 10,000$) the kinematic modelling of spatially resolved spectral lines.[18]

Hence optimisation of sensitivity over spectral dispersion is arguably the hardest compromise to make. However high spectral dispersion must be attained with a grating or grism which splits the light into multiple orders, reducing the amount that reaches a CCD configured to sample a single order. Hence the initial design of FOURIER will consist of a simple prism as is often implemented in combiners for a low dispersion mode. This again is to maximise throughput but has a secondary advantage that it will allow the detector to sample the J, H and K bands simultaneously due to the low linear dispersion across the CCD.

For the detector the SAPHIRA[19] has been selected. The SAPHIRA detector has demonstrated a read noise of less than one electron when operated at a frame rate of one KHz.[20] This allows photon counting at times of order equal to the coherence time.[21] Giving rise to interesting prospects such as operating FOURIER as both a science combiner and fringe tracker simultaneously.[22]

4. THE PRELIMINARY DESIGN

The preliminary layout of FOURIER is presented in figure 1. The beam path from arriving at the beam combiner table to the CCD is as follows: three 13 mm beams are reflected off of a large 250 mm radius parabolic mirror (M1) and pass through the cryostat window before reaching a focus on the slit aligned to spatially filter the beams in the spectral dispersion direction. The beams then continue to a cylindrical mirror (M2) which acts to fold the path and bring the beams in the fringe direction to a focus on the SAPHIRA. Next the light is spectrally dispersed before passing through a cylindrical lens that focuses the beams onto the SAPHIRA in the spectral dispersion direction.

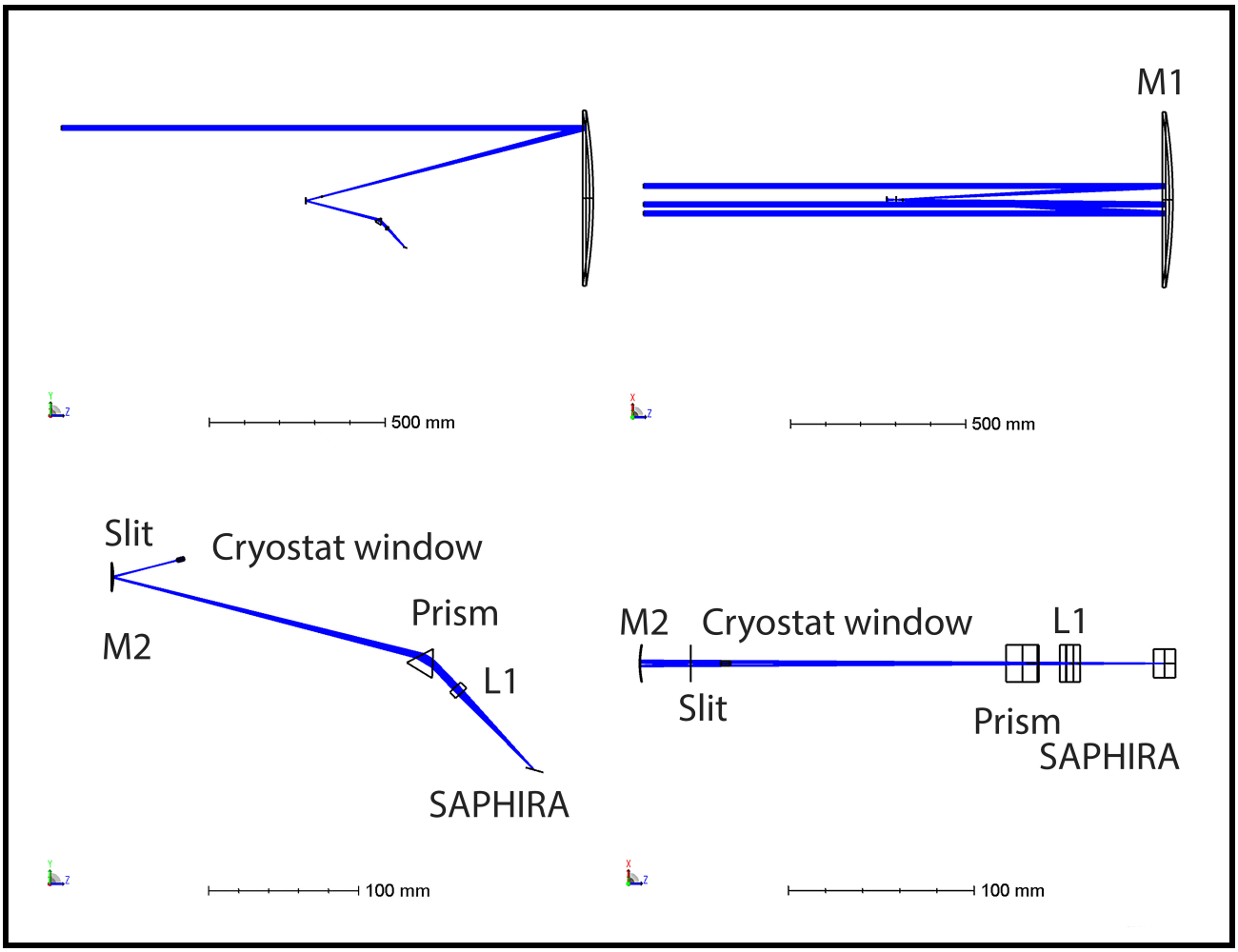

Figure 1. The preliminary layout of FOURIER. Top left: a view of the full combiner in the YZ plane. Top right: in the XZ plane. Bottom left: a view of the inside of the cryostat in the YZ plane. Bottom right: in the XZ plane. The beam propagation is as follows: the three beams reflect off of M1, continuing on to the cryostat window where they come to a focus on the slit. The beams then reflect off of M2 and begin to focus in the interference fringe direction, continuing on to pass through the prism and the second cylindrical component L1, before finally reaching a focus on the SAPHIRA detector.

The current optical components are designed to create appropriately sized fringes for the SAPHIRA's 24 μm pixels. The aim is to minimise the spot size in the spectral dispersion direction to improve spectral resolution. This, combined with the constraint of how many pixels are required to sample the fastest fringe sets the anamorphic factor (of order 20 times) which in turn sets the positions of the cylindrical optical components and the spot size formed by the large parabolic mirror M1. Hence the design is heavily constrained which is the cost of significantly reducing the complexity of FOURIER to achieve greater sensitivity.

4.1 The Slit

The slit is placed at the focus of the large parabola (M1). As an initial guess it is sized such that at 1.75 μm (the centre of the pass band of FOURIER) only the central lobe of the Airy function passes in the spectral dispersion direction where as the entire waveform passes in the interference fringe direction. This leads to a slit width of 244 μm. This however results in parts of the central lobe at longer wavelengths being blocked, reducing the total throughput of the combiner at these wavelengths. At shorter wavelengths the filter allows more than the central lobe to pass and so is not as effective a spatial filter.

A study is required to investigate if this is the ideal slit size. A compromise between the ability to effectively spatially filter at shorter wavelengths while at the same time maximising the throughput at longer wavelengths must be found. This will likely be realised by selecting a error budget for visibility calibration and modelling to find the slit size that produces that level of error at the shorter wavelengths. The possibility of a triangular slit to allow the varying of the slit size if only one or two of the J, H and K bands are of interest for a given observation will be considered if it is found that re-optimizing in this case offers a significant advantage.

4.2 The Anamorphic Stage

The anamorphic stage of FOURIER is comprised of a cylindrical mirror (M2) followed by a cylindrical lens (L1), figure 1. These two components act in conjunction with each other to re-image the slit onto the SAPHIRA detector, magnifying the slit image in the interference fringe direction while de-magnifying the image in the spectral dispersion direction with the focus of both optical components being at the SAPHIRA. A mirror was chosen for the first cylindrical component as mirrors are favoured over lenses due to their largely achromatic properties.

Different focal lengths for each anamorphic stage are also utilised. A focal length of 25 mm was selected for M2 as it was found this was the ideal balance between a long enough focal length to reduce aberrations in the interference fringe direction while still allowing for a short enough beam path from the mirror to a focus on the SAPHIRA that the design could fit in a realistically sized cryostat for a given required magnification in the interference fringe direction. An initial design constrained L1 to have the same focal length as M2 (at the centre of the passband, 1.75μm). However this resulted in a short propagation distance from the lens to the SAPHIRA which in turn gave a low linear dispersion ($\sim$ 0.6 mm from the end of the J band to the end of the K band). To resolve this issue and decrease aberrations a longer focal length of 60 mm was implemented for L1. A longer focal length however reduces the demagnification for the constraint of a fixed path length (fixed by M2) if both directions are to be brought to a focus at the SAPHIRA.

4.2.1 The Prism

The prism is constructed of fused Silica. This is the same material that the GRAVITY combiner uses for its low dispersion mode.[23] This material has been chosen due to its high throughput in the near-infrared. Another reason is due to its large $dn/d\lambda$ value at near-infrared wavelengths for its low refractive index (which reduces the angle of minimum deviation to $\sim 17.5°$).

An additional constraint has been to minimise the size of the cryostat to $\sim$ 300 mm, reducing running costs of FOURIER. This has come at the expense of spectral dispersion, resulting in a small beam size of 5.5 mm incident on the prism. Though as mentioned in section 4.2 the spectral dispersion has been increased by changing the focal length of L1.

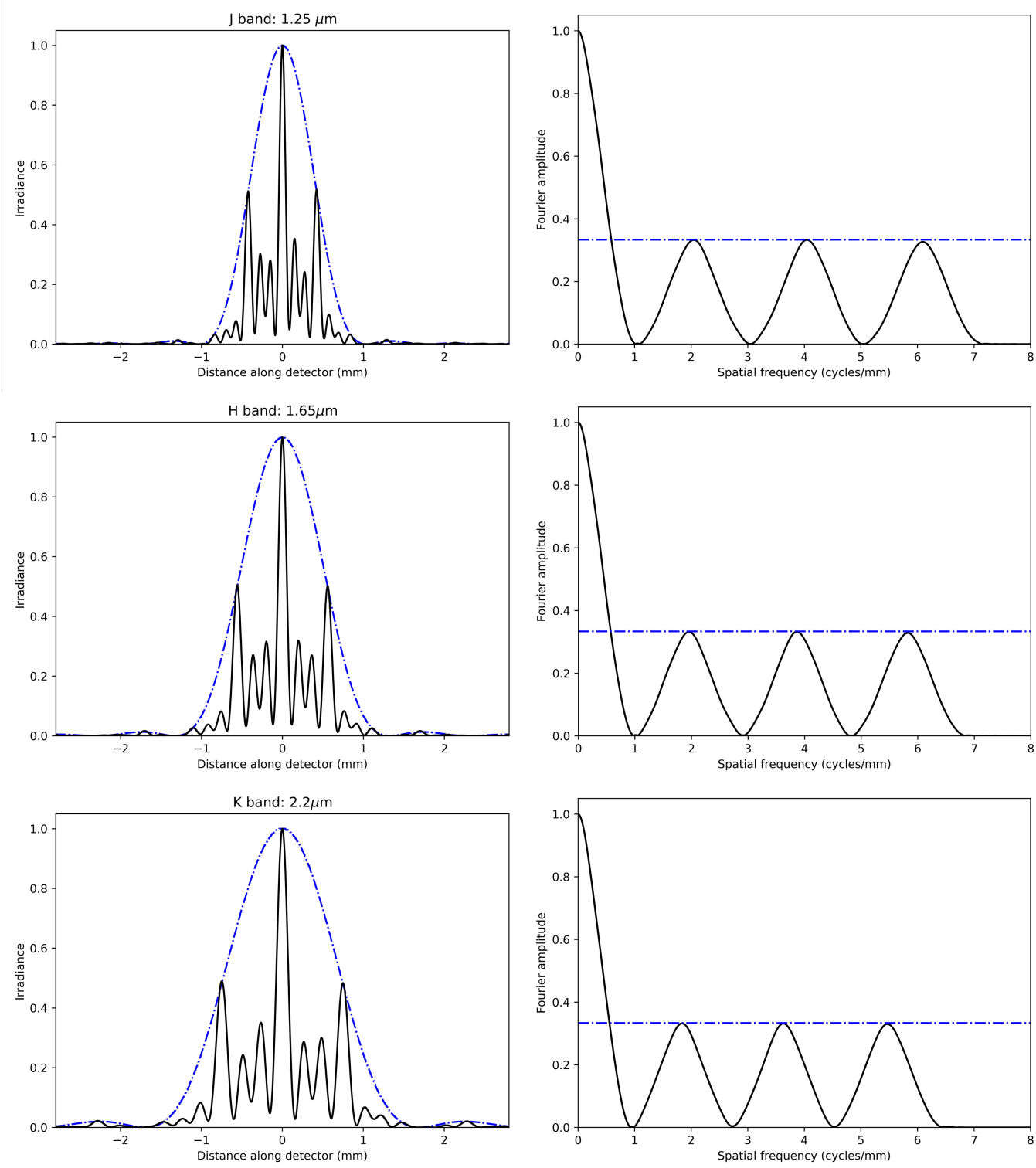

Figure 2. Left: A slice along the interference fringe (simulated by the Zemax physical optics propagation algorithm) on the SAPHIRA detector at the centers of the J, H and K bands. Here the dashed blue line represents the modulating Airy function over the interference fringe. Right: The corresponding modulus of the Fourier transform with the blue dashed line representing the expected height for zero visibility loss.

5. SIMULATED PERFORMANCE

5.1 The Fringe Pattern

The left panels of figure 2 show the resulting fringe pattern across the SAPHIRA detector after propagating through the design at the centres of the J, H and K bands. The right panels show the modulus of the Fourier transform. The size of the modulating Airy function in the interference direction incident on the SAPHIRA detector has been optimised to take advantage of our ability to read out a large number of pixels across the SAPHIRA array. At 2.4 microns this translates to 152 pixels being required to be read out to sample the central lobe or 279 pixels to sample out to the first side lobes of the fringe pattern. The right panels of figure 2 show that the three peaks from the three baselines in the frequency domain are well separated ensuring no cross-talk between baselines at any wavelength. Also of note is that this preliminary design is able to achieve average systematic visibility losses due to the optical components of less than 0.7% with no losses greater than 2% at the centres of the J, H and K bands, this is demonstrated by the blue dashed line representing the expected height for zero visibility loss in figure 2.

5.2 Spectral Resolution

Currently a low spectral resolution mode comprised of a single silica prism has been implemented. While this produces a low spectral dispersion it provides a high throughput, increasing sensitivity. The R values for the current design are presented in table 1.

The spectral focusing lens (L1) was chosen to minimise aberrations with the aim of reducing the spot size at a given wavelength. Increasing the focal length reduces the aberrations in the geometric spot size and has a secondary effect of increasing the linear dispersion of the focused beam on the SAPHIRA detector. To minimise the effects of chromatic aberration the SAPHIRA has been mounted at an angle with respect to the beam. This can be seen in figure 3 where the lower ends and centres of each of the J, H and K bands are shown.

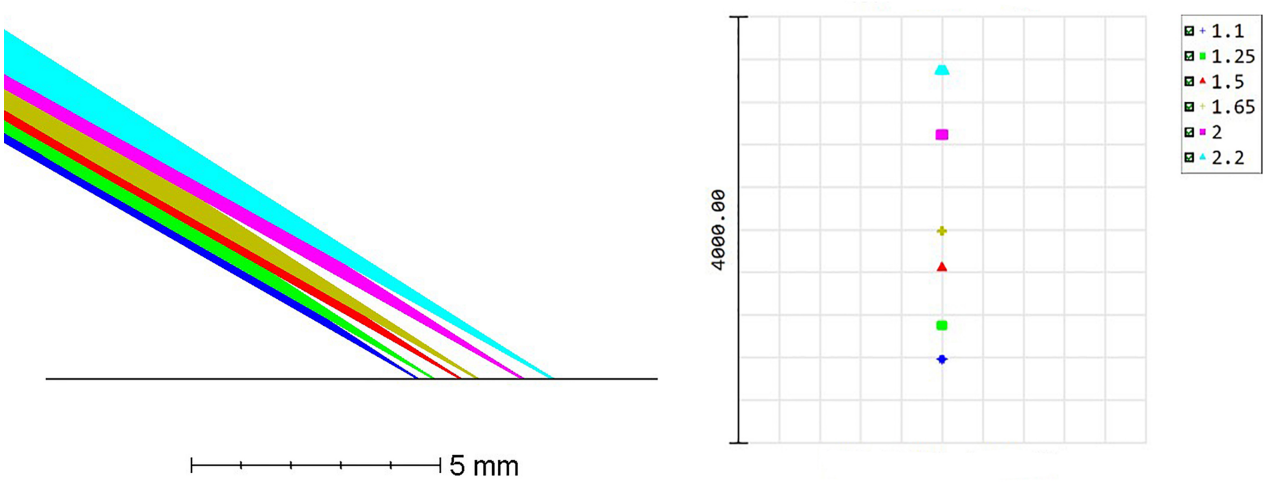

Figure 3. Left: The surface of the SAPHIRA detector showing the spectrally dispersed light incident on the SAPHIRA at the lower ends and centres of each of the J, H and K bands. Right: The spot diagram at the SAPHIRA detector for the same wavelengths. The scale on the right is microns.

5.3 System Throughput

As this is a preliminary design still subject to change we present here a basic throughput analysis to give a rough estimate of the throughput. Here it is assumed that all mirrored surfaces are coated with a protected silver coating which reflects $\sim$ 98% of light in the J, H and K bands. The transmissive components are assumed to be uncoated Infrasil fused silica which gives a transmission of $\sim$ 94% across the bands. More detailed analysis is required to gauge the transmission of the slit however to first order it is assumed that a slit sized to cut

the side lobes of the Airy function at 1.75 μm uniformly transmits 90% of the incident light. Assuming these values results in the throughputs presented in table 1, note this does not include the quantum efficiency of the SAPHIRA detector but mealy the throughput of light reaching the SAPHIRA. These calculations predict a system throughput of order 70%, while this is subject to change as the design becomes more mature this value suggests that FOURIER will be able to achieve a throughput ~ 7 times greater than what is attainable with current generation beam combiners. This throughput coupled with the goal for the MROI interferometer as a whole to reach 13% throughput from the top of the atmosphere to being detected by the CCD[5] will allow the MROI to reach unprecedented levels of sensitivity.

Table 1. The spectral resolution, system throughput and spot size on the SAPHIRA at the centres of the J, H and K bands. The spot size value is based on the SAPHIRA's 24μm pixels. The larger value is along the interference fringe while the smaller is the value perpendicular to this along the spectral dispersion direction.

Band	R	Throughput	Spot size
J	~ 28	72%	86 x 4
H	~ 32	73%	119 x 5
K	~ 61	74%	140 x 6

6. FUTURE WORK

The immediate next step is to further the current layout presented in figure 1 by investigating what improvements can be gained with different optical coatings, especially on the prism surface. A study into the benefits of different transmissive optical materials will also be carried out, particularly for the prism where materials that could potentially provide a larger dispersion will be investigated. As mentioned previously this future design work will also include a study into the ideal slit size for the simultaneous J, H and K band mode.

Alternative layouts will also be studied, for example the use of a cylindrical doublet to replace L1 will be considered, a study into whether the reduced aberrations outweigh the cost of decreased throughput due to the extra optical components will be carried out. A design that utilises off-axis, cylindrical ellipsoidal mirrors in the anamorphic stage is also being considered as this would firstly reduce the number of transmissions required, reducing chromatic aberrations, and secondly may reduce other forms of aberrations as in an ideal case such as design would perfectly re-image the slit onto the SAPHIRA detector.

Different spectral dispersion modes will be considered. While maximising sensitivity is the top priority for FOURIER, a study into the feasibility of higher spectral dispersion modes will be carried out.

Finally a study into the alignment tolerancing of all potential designs and how misalignments will alter the throughput and the visibilities will be conducted before the design phase is completed to ensure that the final design is realistic to construct.

6.1 Beyond FOURIER

FOURIER is *not* intended to be the beam combiner that will operate on the final 10 telescope configuration at the MROI. FOURIER is a quick to build instrument that will be ready to take advantage of the initial three telescope phase due to begin in 2020.[24]

The current outlook is that the final beam combining instrument at the MROI will comprise of two identical five beam combiners supported by a fast switch yard that will allow all baseline and closure phases to be measured in a short time span. FOURIER has been designed with this in mind, thanks to its relative simplicity it should be possible to scale up the design in the future to the five way combiner that will be required for the final configuration.

7. ACKNOWLEDGEMENTS

This material is based on research sponsored by Air Force Research Laboratory (AFRL) under agreement number FA9453-15-2-0086. The U.S. Government is Authorized to reproduce and distribute reprints for Governmental purposes notwithstanding any copyright notation thereon. The views and conclusions contained herein are those of the Authors and should not be interpreted as necessarily representing the official policies or endorsements, either expressed or implied, of Air Force Research Laboratory (AFRL) and or the U.S. Government.

REFERENCES

[1] Rau, G., Paladini, C., Hron, J., et al., "Modelling the atmosphere of the carbon-rich Mira RU Virginis," *aap* **583**, A106 (2015).

[2] Eriksson, K., Nowotny, W., Höfner, S., et al., "Synthetic photometry for carbon-rich giants. IV. An extensive grid of dynamic atmosphere and wind models," *aap* **566**, A95 (2014).

[3] Liljegren, S., Höfner, S., Eriksson, K., et al., "Pulsation-induced atmospheric dynamics in M-type AGB stars. Effects on wind properties, photometric variations and near-IR CO line profiles," *aap* **606**, A6 (2017).

[4] Wittkowski, M., Rau, G., Chiavassa, A., et al., "VLTI-GRAVITY measurements of cool evolved stars: I. Variable photosphere and extended atmosphere of the Mira star R Peg," *ArXiv e-prints* , arXiv:1805.05333 (2018).

[5] Buscher, D., Creech-Eakman, M., Farris, A., et al., "The Conceptual Design of the Magdalena Ridge Observatory Interferometer," *Journal of Astronomical Instrumentation* **2** (2013).

[6] Stee, P., Allard, F., Benisty, M., Bigot, L., et al., "Science cases for a visible interferometer," *ArXiv e-prints* , arXiv:1703.02395 (2017).

[7] Hönig, S. F. and Kishimoto, M., "Dusty Winds in Active Galactic Nuclei: Reconciling Observations with Models," *apj* **838**, L20 (2017).

[8] Weigelt, G., Hofmann, K. H., Kishimoto, M., et al., "VLTI/AMBER observations of the Seyfert nucleus of NGC 3783," *aap* **541**, L9 (2012).

[9] Burtscher, L., Hönig, S., Jaffe, W., et al., "Infrared interferometry and AGNs: Parsec-scale disks and dusty outflows," in [*Optical and Infrared Interferometry and Imaging V*], **9907**, 99070R (2016).

[10] Kishimoto, M., Hönig, S. F., Antonucci, R., et al., "Evidence for a Receding Dust Sublimation Region around a Supermassive Black Hole," *apj* , L36 (Oct. 2013).

[11] Mendigutía, I., de Wit, W. J., Oudmaijer, R. D., Fairlamb, J. R., Carciofi, A. C., Ilee, J. D., and Vieira, R. G., "High-resolution Br γ spectro-interferometry of the transitional Herbig Ae/Be star HD 100546: a Keplerian gaseous disc inside the inner rim," *mnras* **453**, 2126–2132 (2015).

[12] Hone, E., Kraus, S., Kreplin, A., Hofmann, K.-H., Weigelt, G., Harries, T., and Kluska, J., "Gas dynamics in the inner few AU around the Herbig B[e] star MWC297. Indications of a disk wind from kinematic modeling and velocity- resolved interferometric imaging," *aap* **607**, A17 (2017).

[13] Kluska, J., García López, R., and Benisty, M., "The innermost astronomical units of protoplanetary disks," in [*Optical and Infrared Interferometry and Imaging V*], **9907**, 99070V (2016).

[14] Kraus, S., "The interferometric view of Herbig Ae/Be stars," *apss* **357**, 97 (2015).

[15] Fairlamb, J., Oudmaijer, R., Mendigutia, I., et al., "A spectroscopic survey of Herbig Ae/Be stars with X-shooter - ii. Accretion diagnostic lines," *mnras* **464**, 4721–4735 (2017).

[16] Lazareff, B., Berger, J., Kluska, J., et al., "Structure of Herbig AeBe disks at the milliarcsecond scale . A statistical survey in the H band using PIONIER-VLTI," *A&A* **599** (2017).

[17] Kraus, S., "The interferometric view of Herbig Ae/Be stars," *apss* **357** (2015).

[18] Hone, E., Kraus, S., Kreplin, A., et al., "Gas dynamics in the inner few AU around the Herbig B[e] star MWC 297. indications of a disk wind from kinematic modeling and velocity- resolved interferometric imaging," *A&A* **607** (2017).

[19] Finger, G., Baker, I., Alvarez, D., et al., "Evaluation and optimization of NIR HgCdTe avalanche photodiode arrays for adaptive optics and interferometry," in [*High Energy, Optical, and Infrared Detectors for Astronomy V*], **8453**, 84530T (2012).

[20] Mehrgan, L. H., Finger, G., Eisenhauer, F., et al., "Gravity detector systems," in [*Proceedings of the SPIE, Volume 9907, id. 99072F 11 pp. (2016)*], **9907** (2016).

[21] Roddier, F., "The effects of atmospheric turbulence in optical astronomy," *In: Progress in optics. Volume 19. Amsterdam* **19**, 281–376 (1981).

[22] Buscher, D. F., Seneta, E. B., Sun, X., Young, J. S., and Finger, G., "Progress towards photon-counting infrared arrays for interferometry," in [*Optical and Infrared Interferometry and Imaging V*], **9907**, 990716 (2016).

[23] Gravity Collaboration, Abuter, R., Accardo, M., and others., "First light for GRAVITY: Phase referencing optical interferometry for the Very Large Telescope Interferometer," *A&A* **602**, A94 (2017).

[24] Creech-Eakman, M., Romero, V., Payne, I., et al., "A new path to first light for the Magdalena Ridge Observatory interferometer," in [*Optical and Infrared Interferometry and Imaging V*], **9907**, 990705 (2016).